Journal of Materials Chemistry C

PAPER

View Article Online
View Journal | View Issue

Cite this: J. Mater. Chem. C, 2015, 3, 5985

Symmetric naphthalenediimidequaterthiophenes for electropolymerized electrochromic thin films†

V. Figà,[a] C. Chiappara,[a] F. Ferrante,[a] M. P. Casaletto,[b] F. Principato,[a] S. Cataldo,[a] Z. Chen,[c] H. Usta,[d] A. Facchetti*[ce] and B. Pignataro*[a]

Received 17th March 2015,
Accepted 2nd May 2015

DOI: 10.1039/c5tc00746a

www.rsc.org/MaterialsC

A new symmetric naphthalenediimidequaterthiophene (s-NDI2ODT4) was synthesized and exhibited the capability to electropolymerize alone or with EDOT affording polymers with controlled donor/acceptor monomer ratios. s-NDI2ODT4-EDOT-based copolymers showed low band gaps, wide optical absorption ranges extending to the near IR region, tuned electrical properties, thin-film surface morphology and hydrophilicity as well as high coloration efficiency in electrochromic devices.

Introduction

Conjugated polymers endowed with electron-withdrawing and electron-donating moieties have attracted great interest because of their promising optical and electronic properties.[1] For this reason, several research groups have addressed their efforts towards the engineering design and synthesis of new push–pull systems to be used in organic opto-electronic devices. Several of these systems contain thiophene rings, such as alkyl- and alkoxy-oligothiophenes and ethylenedioxythiophene (EDOT), because of their strong electron-donor character.[2] Recently, derivatives of perylenes and naphthalenes have been employed as electron-accepting moieties for realizing semiconducting small-molecules and polymers.[3] Push–pull co-polymers comprising naphthalenediimide (acceptor) and thiophene (donor) derivatives have shown high air-stability, good processability, low band gap, and large electron mobilities,[4] principally due to their substantial crystalline structure or ordered supramolecular packing.[5] Several combinations of naphthalene derivatives and thiophene-based donor groups have been reported in the literature and their transport properties have been studied by several groups.[6] Naphthalenediimide-based polymers have also been employed in different kinds of devices. For instance, poly{[*N*,*N*′-bis(2-octyldodecyl)-naphthalene-1,4,5,8-bis(dicarboximide)-2,6-diyl]-*alt*-5,5′-(2,2′-bithiophene)} (P(NDI2OD-T2)) together with poly(3-hexylthiophene-2,5-diyl) (P3HT) has been employed in very high fill factor solar cells.[7] P(NDI2OD-T2) and poly(*N*,*N*′-dialkylperylenedicarboximide-dithiophene) (P(PDI2OD-T2)) have been used for fabricating bottom and top gate OTFTs with mobilities up to 0.45–0.85 $cm^2 V^{-1} s^{-1}$,[4b] and more recently surpassing 2.5 $cm^2 V^{-1} s^{-1}$.[8] P(NDI2OD-T2) allowed realizing monolayer polymeric field effect transistors[9a] as well as vertical transistors.[9b] Furthermore, molecules based on 1,4,5,8-naphthalene-carboxylic-diimide with thiophene substituents have been studied and the effect of the number of thiophene moieties between two naphthalene units on the polymeric optic and electronic properties has been investigated.[9] More recently, the polymer P(NDI-TVT) showed field-effect electron mobilities as high as 1.5–1.8 $cm^2 V^{-1} s^{-1}$.[10]

On the other hand, the combination of strong electron-donor and self-structuring effects of EDOT with electron accepting systems has been employed as a powerful tool for the design and synthesis of π-conjugated copolymers with a diverse range of optical and electro-optical properties.[11] Thus, associating EDOT with strong electron-withdrawing building blocks enabled rigidified π-structures with improved planarity and greatly reduced band gaps.[12] For instance, copolymers achieved by polymerization of EDOT with electron acceptor units such as cyanovinylene, thieno[3,4-*b*]pyrazine or benzo[1,2-*c*:4,5-*c*′]bis[1,2,5]thiadiazole enabled bandgaps from ∼1.50 eV to as low as ∼0.40 eV.[12] Interestingly, systems bearing EDOT have been employed to synthesize copolymers with electrochromic behaviour extending

[a] Dipartimento di Fisica e Chimica, Università di Palermo, V.le delle Scienze ed. 17, 90128, Palermo, Italy. E-mail: bruno.pignataro@unipa.it; Fax: +39-091-590015; Tel: +39-09123897983
[b] Istituto per lo Studio dei Materiali Nanostrutturati (ISMN), Consiglio Nazionale delle Ricerche (CNR), via Ugo La Malfa, 153, 90146 Palermo, Italy
[c] Polyera Corporation, 8045 Lamon Avenue, Skokie, IL 60077, USA. E-mail: afacchetti@polyera.com
[d] Department of Materials Science and Nanotechnology Engineering, Abdullah Gül University, Kayseri, Turkey
[e] Center of Excellence for Advanced Materials Research, King Abdulaziz University, Jeddah 21589, Saudi Arabia

† Electronic supplementary information (ESI) available: Synthesis of symmetric NDIT systems and characterization; oxidation of NDI2ODT4 and EDOT; cyclic voltammetry during electropolymerization; polymerization kinetics; DFT calculations; optical band gaps; thin film morphology and solvent effects; XPS of the solid supported thin films; electrical measurements; electrochromic properties of PNDI2ODT4 thin films; contact angle measurements; effect of monomer reduction; effect of thermal annealing on copol[2] morphology; and references. See DOI: 10.1039/c5tc00746a

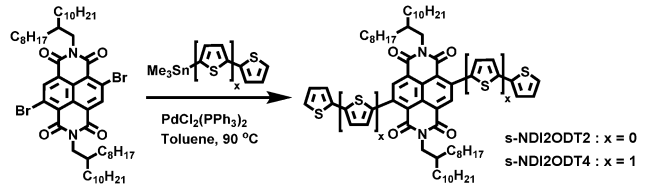

Scheme 1 Chemical structure and synthesis of s-NDI2ODT2 and s-NDI2ODT4.

into the IR region.[13] However, very few studies have investigated the electrochromic properties of naphthalenediimide-based polymers, the most promising achieving polymers with good stability, high transmissivity and high coloration efficiency.[14] Interestingly, both naphthalenediimide with thiophene substituents and EDOT[15] displayed low oxidation onset potentials which allow their electrochemical polymerization in common organic solvents.

In this work, we designed and synthesized two novel symmetric naphthalenediimidethiophenes, namely *N*,*N*′-bis(2-octyldodecyl)-2,6-bis(2-thienyl)naphthalene-1,4,5,8-bis(dicarboximide) (s-NDI2ODT2) and *N*,*N*′-bis(2-octyldodecyl)-2,6-bis(5-(thioph-2-yl)thiophen-2-yl)-naphthalene-1,4,5,8-bis(dicarboximide) (s-NDI2ODT4) (Scheme 1). Their symmetric structure has been designed to allow for regioregular electropolymerization with EDOT. For s-NDI2ODT4, electropolymerized films with new structural and optoelectronic properties along with electrochromic devices are achieved and discussed.

Results and discussion

Monomer synthesis and characterization

The synthesis of s-NDI2ODT2 and s-NDI2ODT4 was carried out under argon by reacting a mixture of 2-(trimethylstannyl)thiophene and 5-(trimethylstannyl)-2,2′-dithiophene with, respectively, NDI2OD-Br_2 and $Pd(PPh_3)_2Cl_2$ in anhydrous toluene. Upon cooling to room temperature, the reaction mixtures have been diluted with chloroform and then washed with water, dried over anhydrous sodium sulfate, and concentrated on a rotary evaporator. The residues were subjected to column chromatography on silica gel with a mixture of chloroform:hexane as an eluent, leading to an orange (s-NDI2ODT2) or a purple (s-NDI2ODT4) solid as the product (Scheme 1). Synthetic and characterization details can be found in the ESI.† From optical absorption spectra in acetonitrile : dichloromethane solution (2 : 3; v : v), the maximum absorption for s-NDI2ODT2 and s-NDI2ODT4 are located at 250 nm and 300 nm, respectively. Cyclic voltammetry (CV) measurements carried out in acetonitrile : dichloromethane solution (2 : 3; v : v) containing 10^{-2} M $LiClO_4$ and 10^{-4} M monomers indicate the oxidation onset potentials located at +1.6 V and +1.15 V for s-NDI2ODT2 and s-NDI2ODT4, respectively, and oxidation peaks located at +1.8 V and +1.24 V, for s-NDI2ODT2 and s-NDI2ODT4 respectively. Reversible oxidations have not been observed, however, the onset of these processes has shifted to more positive potentials for s-NDI2ODT2 *versus* s-NDI2ODT4. This result corroborates that the presence of a greater number of electron-rich thiophene units facilitates oxidation.

Electropolymerization

We performed electrochemical polymerization of the pristine NDI-based monomers alone and in the presence of EDOT to modulate the polymer properties. Our results show that while s-NDI2ODT2 did not electropolymerize under several conditions, s-NDI2ODT4 alone or in the presence of EDOT showed the efficient formation of solid thin films supported on the electrode. These results can be rationalized by deactivation of the thiophene pendant radical cation of s-NDI2ODT2 due to the contiguity of the strongly electron-accepting NDI moiety. Deactivation of electropolymerization in electron-depleted moieties has been reported for other classes of compounds.[16] On the other hand, in s-NDI2ODT4 the external thiophenes may be easily polymerized since they are spaced from the NDI unit by the internal thiophene. Thus, the new compound s-NDI2ODT4 represents a new entry to achieve electropolymerization of NDI2OD-oligothiophene-based systems. Electropolymerized PNDI2ODT4, PEDOT and $(NDI2ODT4)_m$–$(EDOT)_n$ copolymers with different ratios were obtained by CV (Ag/AgCl, 3.5 M KCl). For all the systems, the electrode potential has been increased from the open circuit value to +1.3 V and reversed to the open circuit value for several cycles.

Fig. 1 displays CV scans for s-NDI2ODT4 in acetonitrile:dichloromethane solution (2 : 3; v : v) containing 10^{-2} M $LiClO_4$ and 10^{-4} M monomer at a potential scan rate of 50 mV s^{-1}. The first cycle presents an oxidation potential onset of +1.15 V that indicates the potential at which the monomer starts to be oxidized. The current reaches a peak value at +1.24 V. The oxidation onset lowered with the number of cycles suggesting that the previously formed oligomers are easier to oxidize than the monomer. As the CV scan continues, the polymer film is formed at the working electrode. The film thickness increases with the number of CV cycles as suggested by the increase of the current. CV curve shapes differ when going from the polymerization of NDI2ODT4 or EDOT to that of $(NDI2ODT4)_m$–$(EDOT)_n$, suggesting successful copolymerization and incorporation of both monomers. Three s-NDI2ODT4 : EDOT molar ratios have been used affording the following copolymers: copol[1] (10 : 1), copol[2] (1 : 1), and copol[3] (1 : 10) (Fig. 2).

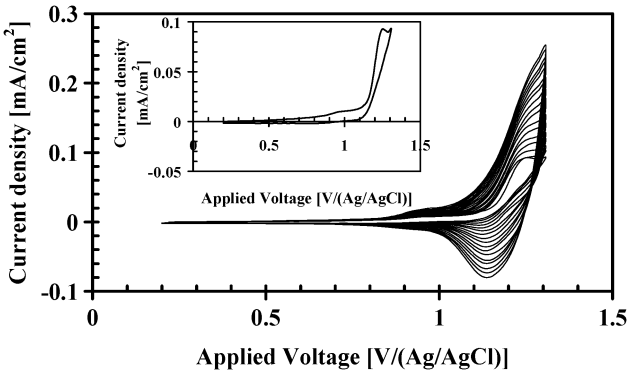

Fig. 1 Cyclic voltammetry of a 10^{-4} M acetonitrile : dichloromethane solution (2 : 3; v : v) of s-NDI2ODT4 containing 10^{-2} M $LiClO_4$, recorded using glassy carbon (S = 0.07 cm^2) as a working electrode. Inset: first cycle of the CV plot.

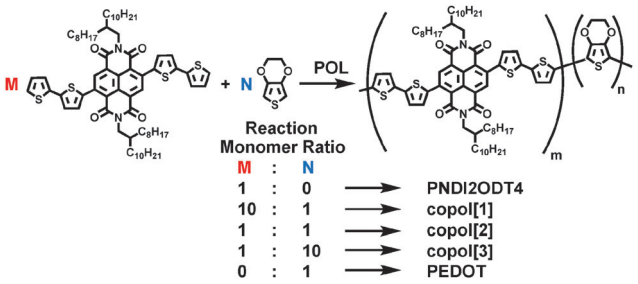

Fig. 2 Chemical structure of the NDI2OT4:EDOT electropolymerized copolymers with M and N indicating the monomer loading ratios, and m and n the number of incorporated NDI2OT4 and EDOT units in the structure, respectively.

Both homopolymer and copolymer thin films were chemically characterized by XPS analysis (Fig. 3). As expected, the oxygen, carbon, nitrogen and sulphur elements are present in the wide spectra of all the thin films. Fig. 3a shows the XPS C1s spectra of different electropolymerized thin films. The C1s peak shape of the copol[1] and copol[3] copolymers closely resembles that of predominant PNDI2ODT4 and PEDOT, respectively. The C1s peak of the copol[2] copolymer appears quite different being located in-between the two homopolymers. As resulted from the curve-fitting procedure, the XPS C1s spectrum of copol[2] can be deconvoluted by four components, as reported in Fig. 3b. The component located at a binding energy (B.E.) of 284.5 eV is assigned to C–C, C=C, and C–H bonds; the component at B.E. = 285.9 eV is attributed to C–S and C–N bonds; the component located at B.E. = 286.7 eV corresponds to the presence of C–O bonds and the component at B.E. = 288.3 eV is typical for N–C=O bonds.[31] The results of the XPS C1s curve-fittings of the other samples are reported in the ESI.† By considering the surface C/S atomic percentage ratios (see Table 1) and the C 1s deconvoluted peaks (see ESI†), it is possible to establish the actual monomer incorporation in the $(NDI2ODT4)_m$–$(EDOT)_n$ copolymers as a function of the monomer concentration ratios employed for the electropolymerization (Fig. 2). Thus, in addition to the PNDI2ODT4 and PEDOT homopolymers, we reasonably formed $(NDI2ODT4)_m$–$(EDOT)_n$ copolymers with $4 < m < 8$ and $n = 1$ in the case of copol[1], $m = 1$ and $4 < n < 5$ for copol[2], and $m = 1$ and $n = 8$ for copol[3]. XPS shows that the increase in the EDOT content leads to a higher surface oxygen content, which should indicate a more hydrophilic film as also observed by water contact angle experiments. The water contact angle ranges from 107.7° for PNDI2ODT4 to about 65.35° for copol[3] (see ESI†).

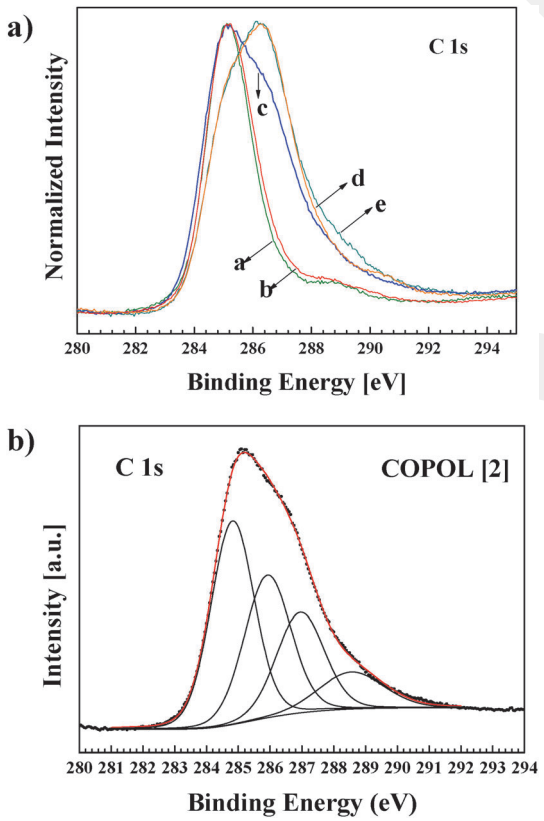

Fig. 3 (a) Normalized C1s XPS spectra of the electropolymerized thin films: (a) PNDI2ODT4; (b) PEDOT; (c) copol[2]; (d) copol[1] and (e) copol[3], all electrodeposited onto ITO/PET substrates. (b) XPS curve-fitting of the C 1s photoelectron spectrum of the copol[2] thin film.

Polymer electronic structure

In order to investigate the nature of the electronic transitions, molecular models of NDI2ODT4–$(EDOT)_n$–NDI2ODT4, (n = 0, 1, 4), $(EDOT)_n$ (n = 8, 12, 16) and $(EDOT)_n$–NDI2ODT4–$(EDOT)_n$ (n = 3–8) systems were subjected to full geometry optimization and subsequent TDDFT calculations. The computed molecular geometries are qualitatively similar to those reported for analogous species, such as the P(NDI2OD-T*) series[6,17] – the NDI moiety and the bonded thiophene-derivative chain lie in planes tilted by approximately 50°, and this strongly reduces electron conjugation throughout the polymer chain. The results obtained for the first three singlet–singlet vertical transitions are reported in Table S1 of the ESI† together with their oscillator strengths. The transition at lower energy in the investigated structures has a charge-transfer (CT) nature, with the electron density migrating from the π-system of the EDOT chain to the π-system of NDI2ODT4. The HOMO and the LUMO are the molecular orbitals most largely involved in this CT transition, but in the larger systems several other quasi-degenerate orbitals can be observed with sensible weights. In particular, while the inclusion of one EDOT between two NDI2ODT4 units leads to a

Table 1 XPS surface chemical quantitative analysis of the electropolymerized thin films. Elemental composition is expressed as an atomic percentage[a]

Sample	C 1s	O 1s	N 1s	S 2p	In 3d	Sn 3d
PNDI2ODT4	70.5	18.4	2.0	3.1	5.3	0.7
Copol[1]	81.9	11.0	1.9	4.7	0.4	—
Copol[2]	67.3	23.4	1.4	7.1	0.7	—
Copol[3]	68.6	23.8	0.8	6.5	0.3	—
PEDOT	58.4	33.4		7.8	0.4	—

[a] In3d and Sn3d photoelectron signals originate from the ITO substrate. No ClO^{4-} doping anions have been observed by XPS in these samples.

slight energy decrease of the $S_0 \rightarrow S_1$ CT transition, in NDI2ODT4–$(EDOT)_4$–NDI2ODT4, the appearance of a second intense transition ($S_0 \rightarrow S_3$) can be noted, involving the EDOT π-system. The $S_0 \rightarrow S_2$ transition is forbidden or very weak in the oligomers. Thus, in the NDI2ODT4–$(EDOT)_n$–NDI2ODT4 series, the $S_0 \rightarrow S_1$ transitions are found at 2.472, 2.385, and 2.225 eV for n = 0, 1, and 4, respectively. In the same way, the insertion of one NDI2ODT4 unit into EDOT for the $(EDOT)_n$–NDI2ODT4–$(EDOT)_n$ (n = 3–8) series causes the occurrence of a CT transition at energy (from 2.212 eV for n = 3 to 2.151 eV for n = 8) lower than the $\pi \rightarrow \pi^*$ transition (from 2.821 eV for n = 3 to 2.520 eV for n = 8). In other words, when the orbital conjugation in PEDOT is interrupted by NDI2ODT4 units, the CT transition shifts to a higher wavelength (Fig. 4a). So, this transition energy could be modulated by the appropriate choice of the NDI2ODT4–EDOT ratio in the copolymer. Finally by comparing the HOMO and the LUMO representations of the EDOT–NDI2ODT4–EDOT molecule, a different phase is observed in one of the linkage points (see ESI†). Accordingly, this result would suggest that the polymer is a direct gap semiconductor.[18]

Fig. 4b displays the UV-Vis absorption spectra of PNDI2ODT4 and PEDOT homopolymers together with those of copol[1], copol[2] and copol[3]. The convolution of the PEDOT and PNDI2ODT4 spectra does not show the same peak shapes observed for the copolymers as a further proof of the successful copolymerization process. In particular, the spectra of PNDI2ODT4 display two transition bands – the high energy band (350–450 nm) may be attributed to excited states more localized on thiophene units ($\pi \rightarrow \pi^*$ transition), whereas the low energy band (550–800 nm) can be assigned to an intramolecular charge transfer transition.[6] Electropolymerized PEDOT shows just a broad absorption band at long wavelengths typical for the oxidized form.[19] In addition to the NDI2ODT4 π–π^* and CT transition bands, copol[2] presents a shoulder in the 440–500 nm region that can be ascribed to new components typical for the copolymer system. This shoulder increases with the EDOT amount. By considering the PNDI2ODT4 homopolymer and copol[2], it is possible to observe a red shift of the CT transition band as well as a spectral absorption up to the near IR region as an indication that by adding EDOT units to NDI2ODT4 a band gap reduction occurs. A red shift in the CT transition band cannot be otherwise observed for further increased amount of EDOT because of the overlapping of the broad absorption band at long wavelengths. Interestingly, by opportunely modulating the monomer ratio (see for instance, copol[2]) it is possible to obtain copolymers with a wide optical absorption range with a solar spectrum coverage including both visible components and the near IR region as confirmed by the spectroscopic investigation up to about 1020 nm.

The optical band gap has been calculated under the above hypothesis of direct optical transitions,[20] by plotting $(\alpha h\nu)^2$ *vs.* $h\nu$, fitting the straight portion and extrapolating to $(\alpha h\nu)^2 = 0$. In particular, by increasing the EDOT content in the copolymer systems, we notice a decrease of the optical band gap spanning from 1.5 eV to 1.15 eV for copol[1] and copol[2], respectively, (see ESI†). This trend is consistent with the DFT calculations reported above and the literature results of EDOT–NDI copolymers.[21] This result suggests that by the NDI2ODT4–EDOT copolymerization we can design copolymers with appropriate optical properties including band gap modulation and controlled optical absorption in the near UV and near IR regions.

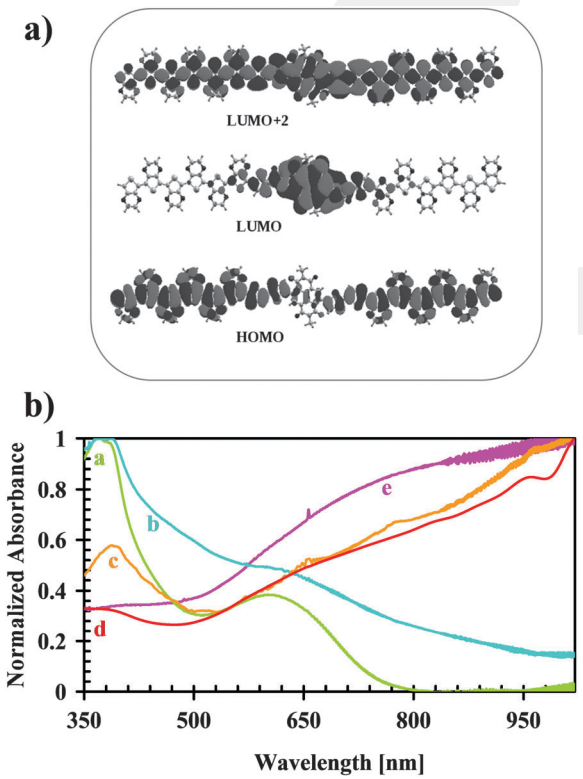

Fig. 4 (a) DFT computations of $(EDOT)_6$–NDI2ODT4–$(EDOT)_6$ showing selected MO topologies. (b) Optical absorption spectra of PNDI2ODT4 (a), copol[1] (b), copol[2] (c), copol[3] (d) and PEDOT (e).

Polymer film morphology and charge transport

Fig. 5 shows scanning electron microscope (SEM) images of selected electropolymerized films, highlighting the morphological changes upon EDOT incorporation. Thus, the PNDI2ODT4 film is quite compact with a surface morphology characterized by the particle grain size of 8–20 nm, whereas copol[1] displays a globular structure with 10–40 nm size particles. By increasing the EDOT amount, the copol[2] film is mainly porous with features spanning 10–180 nm. Copol[3] displays a mixed morphology with reduced porous features (15–100 nm large) together with globular nanoparticles of 10–90 nm in size. Finally, PEDOT thin films show branched features with the presence of a few pores with a diameter of 30–250 nm (for further morphological

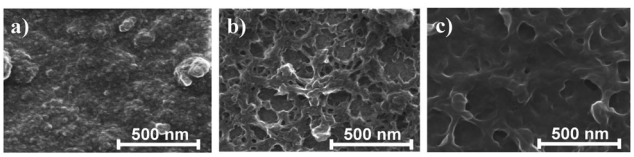

Fig. 5 SEM images of PNDI2ODT4 (a), copol[2] (b), and PEDOT (c).

details, see ESI†). The data shown above indicates that the incorporation of EDOT into NDI2ODT4 gives rise to branched thin film supramolecular structures with the formation of porous features. For a number of applications, it may be desirable to achieve more smooth film surfaces. By thermal annealing of the thin films at about 160 °C for 40 minutes surface smoothing has been obtained (see ESI,† Fig. S9b, about 20% decrease in roughness of copol[2] as determined by AFM).

Charge transport measurements of the electropolymerized films (400–500 nm thick) using a mercury probe indicate a progressive trend from a rectifying behavior for PNDI2ODT4 to the degenerate semiconducting behavior for PEDOT. In particular, whereas electrodeposited PEDOT gives an ohmic behavior with a conductivity of about 6 S cm^{-1},[22] copol[2] leads to an ohmic behavior (conductivity of about 10^{-5} S cm^{-1}) at a low bias potential and a space charge limited current (SCLC) regime at higher bias obeying the $I = KV^2$ law. A similar behavior is observed for copol[1] but with conductivity in the order of 10^{-6} S cm^{-1}, whereas PNDI2ODT4 shows a threshold potential of about 1.4 V (Fig. 6; see ESI† for further details). From eqn (1)[23]

$$J_{SCL} = \frac{9}{8}\varepsilon_0\varepsilon_r\mu\frac{V^2}{d^3} \quad (1)$$

which governs the transport in a space-charge limited current regime, (where J_{SCL} = space charge limited current; V = voltage; d = thickness, μ = charge carrier mobility, ε_0 = permittivity in vacuum, and ε_r = relative static permittivity), the carrier mobility values of copol[1] and copol[2] were found to be 2.5×10^{-7} cm^2 V^{-1} s^{-1} and 1.7×10^{-6} cm^2 V^{-1} s^{-1}, respectively, using SCLC measurements. These results suggest that by increasing the EDOT moiety content, the copolymers exhibit higher carrier mobilities in agreement with the greater content of the electron-rich EDOT.

Optoelectronic properties

From cyclic voltammetric experiments, we have found that the onset oxidation potential of EDOT rich copol[2] and copol[3] polymers is ~1.5 V and it is larger than that of both PEDOT (0.95 V) and PNDI2ODT4 (1.15 V). This result indicates that copolymer-based thin films are more stable toward electrochemical oxidation than the respective homopolymers due to a strong coupling between the two different donor–acceptor monomer units. This effect has been observed for some thiophene-based copolymer classes and monomer mixtures.[24] The optoelectronic properties of homopolymer and copolymer thin films were investigated for understanding the changes in transmittance due to different redox states. For this reason, films of about 200 nm were electrodeposited onto transparent ITO/PET electrodes (2.4 cm^2). The characterization was performed by employing 0.1 M $LiClO_4$ in CH_3CN and by using a two-electrode configuration in a 1 cm path length cuvette endowed with quartz windows. For the estimation of the optical contrast and response time, we applied square wave potentials (SWP), and transmittance *vs.* time curves were recorded at suitable wavelengths (λ). The best conditions (potential and λ) were identified by recording the absorption spectra of the films at different polarization potentials.

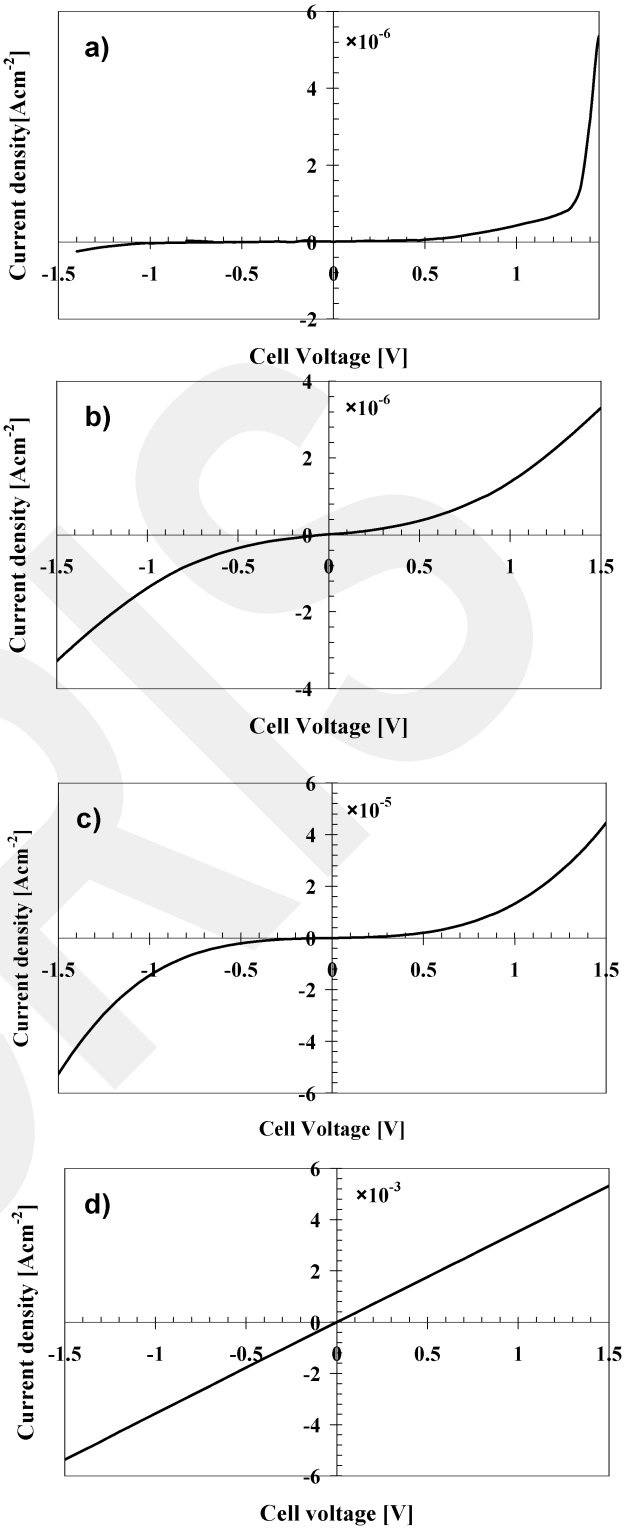

Fig. 6 Current density–voltage plots of PNDI2ODT4 (a), copol[1] (b), copol[2] (c), and PEDOT (d).

The PNDI2ODT4 polymer displays the highest optical contrast of 19% between +0.8 V and −0.8 V and at 900 nm (Fig. 7a); furthermore, it displays high stability in the explored time and potential ranges. It appears green and light brown in the oxidized

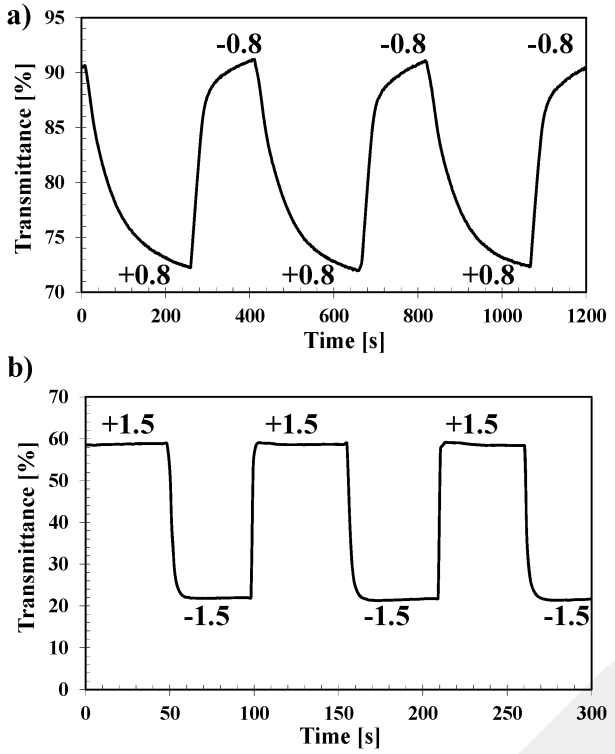

Fig. 7 Transmittance *vs.* time plots in CH_3CN (0.1 M $LiClO_4$) for (a) PNDI2ODT4 thin films at 900 nm and (b) copol[2] thin films at 580 nm.

(+0.8 V) and reduced (−0.8 V) states, respectively. Note, this polymer is also green in the neutral state. By considering the electrochemical charge required for a complete switching and the optical density at 900 nm, a coloration efficiency of 302 cm^2 C^{-1} was calculated. This value is comparable with the coloration efficiency of novel classes of poly(ether-imide)s.[25] PNDI2ODT4 exhibits slow response times compared to other poly(naphthalene) derivatives.[26] Thus, it requires 110 seconds for shifting from the oxidized to the reduced state and 250 seconds for the inverse process, suggesting different charge transfer kinetics for the oxidized and reduced PNDI2ODT4 species. The presence of EDOT moieties in the NDI2ODT4 based chain improves the electrochromic response of the resulting copolymers in terms of both optical contrast and response time. Thus, copol[2] exhibits an optical contrast up to 37% at 580 nm and response times of 13 (ox → red) and 15 (red → ox) seconds (Fig. 7b) under a square wave potential between + 1.5 V and −1.5 V. By increasing the EDOT amount, as it is in the case of copol[3], the optical contrast saturates to similar values but at 588 nm. This shift could be attributed to the greater EDOT content since the PEDOT highest optical contrast is recorded at ∼600 nm.[28] Also, these values are ∼10% higher than those measured for different electrochemically synthesized EDOT-naphthalene based copolymers, which have displayed an optical contrast of 26%.[29] Copol[1] exhibited the same optical contrast of PNDI2ODT4 at 900 nm and shorter response times but it has appeared unstable (see ESI†). Table 2 shows the performance parameters for different electropolymerized systems.

Table 2 Summary of the electrochemical and optical data for different electropolymerized thin films[a]

Polymer	Oxidation onset [V/(Ag/AgCl)]	λ_{max} [nm]	$E_{g,opt}$ [eV]	Response time [s]	ΔT [%] at ±1.5 V
PNDI2ODT4	1.15	370	1.71	108 o → r 250 r → o	19[b]
Copol[1]	1.15	370	1.50	50 o → r 20 r → o	20[b]
Copol[2]	1.50	390	1.15	13 o → r 15 r → o	37
Copol[3]	1.50	N.D.	N.D.	10 o → r 13 r → o	30
PEDOT	0.95	N.D.	N.D.	12 o → r 10 r → o	34

[a] For copol[3] and PEDOT, it was not possible to determine precise λ_{max} and optical band gap ($E_{g,opt}$) values (see ESI). [b] For PNDI2ODT4 and copol[1], ΔT% has been evaluated by applying ±0.8 V.

Clearly, the optical contrast and the response time depend on the copolymer chemical composition, thus giving a range of possible applications for these systems. In particular, while the response time and transmittance values of PNDI2ODT4 may be of interest for smart windows or optical filters,[27] the lower response time and higher optical contrast of copol[2] and copol[3] are interesting for simple passive matrix displays.[27]

The copolymers with the best electrochromic performances were employed for the fabrication of solid state electrochromic devices (ECD). Thus, copol[2] and copol[3] electrodeposited onto ITO/PET electrodes were sandwiched with a second ITO/PET electrode using a polymethylmethacrylate (PMMA)-based gel electrolyte (Fig. 8a). These devices were subjected to a square wave potential between ±1.5 V, and the transmittance *vs.* time plots have been recorded by irradiation at 580 nm and 588 nm, respectively. The potential range from +1.5 V to −1.5 V was used since it enables the highest switching rate and the maximum optical contrast along with stability.

In particular, copol[2] (Fig. 8b) and copol[3] based ECDs showed an optical contrast of 22% and 29%, respectively. The response times of these devices are about 15 seconds from reduced to oxidized states. In Fig. 8b (as for 7a) the potential switching from the oxidized to the reduced states occurs in about 200 s without reaching a complete saturation, which requires a longer time but with negligible (<3%) ΔT gain. The stability of copol[2] and copol[3] based ECDs was evaluated by measuring the optical change in the time domain at 580 nm and 588 nm, respectively. As reported in Fig. 8b preliminary data suggest stability for copol[2], the optical contrast being constant in time as it maintains the same value of transmittance under the applied voltages. Copol[3] based ECDs showed reduced stability with respect to those with Copol[2] as indicated in Fig. S13b, (ESI†). The substantial stability of copol[2] based ECDs in the explored time ranges suggests that they are promising materials for different electrochromic applications.

Conclusions

In conclusion, we have identified the s-NDI2ODT4 monomer as a very attractive system for developing new electropolymerized

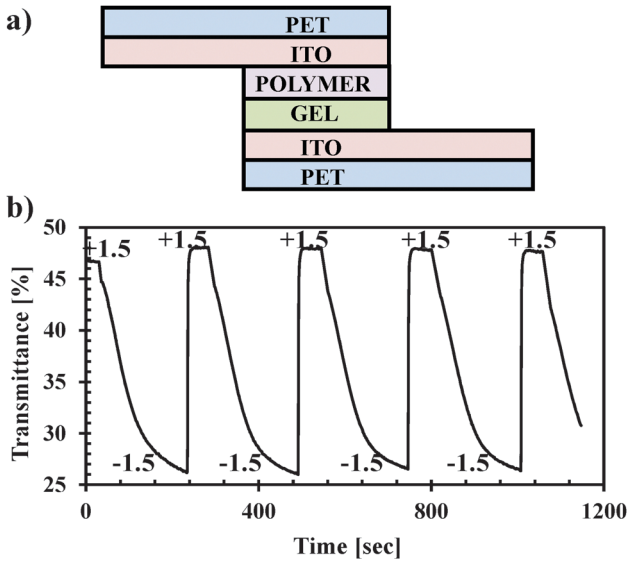

Fig. 8 (a) Solid state ECD configuration and (b) transmittance *vs.* time plots of a representative copol[2]-based ECD.

naphthalenediimide-based copolymers with EDOT having controlled monomer ratios. This approach allows copolymers with a modulation of fundamental properties including the oxidation onset, band gap, optical absorption, carrier mobility, surface hydrophilicity, and film morphology. Among the NDI derivatives investigated to date, these systems exhibit a very low band gap, wide optical absorption range with the solar spectrum coverage up to the near IR region, and high coloration efficiency. Furthermore, we developed interesting electrochromic devices with tuned response time and optical contrast. The physical properties of s-NDI2ODT4 based copolymers might be of interest for other applications including photovoltaics, sensors and biosensors.

Experimental

Synthesis of symmetric NDIT systems

Preparation of *N,N′*-bis(2-octyldodecyl)-2,6-bis(2-thienyl)-naphthalene-1,4,5,8-bis(dicarboximide) (NDI2OD-T1). Under argon, a mixture of NDI2OD-Br_2 (280.0 mg, 0.28 mmol), 2-trimethylstannylthiophene (400.0 mg, 1.62 mmol), and $Pd(PPh_3)_2Cl_2$ (28.0 mg, 0.04 mmol) in anhydrous toluene (20 mL) was stirred at 90 °C for 22 h. Upon cooling to room temperature, the reaction mixture was diluted with chloroform (100 mL), and the resulting mixture was washed with water (80 mL × 2), dried over anhydrous sodium sulfate (Na_2SO_4), and concentrated on a rotary evaporator. The residue was subjected to column chromatography on silica gel with a mixture of chloroform : hexane (3 : 2, v/v) as an eluent, giving an orange solid as the product (240.0 mg, 85.2%). ^{1}H NMR ($CDCl_3$ 500 MHz): δ: 8.77 (s, 2H), 7.57 (d, J = 5.0 Hz, 2H), 7.31 (d, J = 3.5 Hz, 2H), 7.21 (m, 2H), 4.07 (d, J = 7.5 Hz, 4H), 1.95 (m, 2H), 1.18–1.40 (m, br, 64H), 0.84–0.88 (m, 12H).

Preparation of *N,N′*-bis(2-octyldodecyl)-2,6-bis(5-(thioph-2-yl)thiophen-2-yl)naphthalene-1,4,5,8-bis(dicarboximide) (NDI2OD-T2). Under argon, a mixture of NDI2OD-Br_2 (1.00 g, 1.02 mmol), 5-(trimethylstannyl)-2,2′-dithienyl (1.34 g, 4.07 mmol), and $Pd(PPh_3)_2Cl_2$ (0.095 g, 0.14 mmol) in anhydrous toluene (60 mL) was stirred at 90 °C for 16 h. Upon cooling to room temperature, the reaction mixture was diluted with chloroform (100 mL), and the resulting mixture was washed with water (100 mL), dried over anhydrous sodium sulfate (Na_2SO_4), and concentrated on a rotary evaporator. The residue was subjected to column chromatography on silica gel with a mixture of chloroform : hexane (3 : 2, v/v) as an eluent, giving a purple solid as the product (0.85 g, 72.0%). ^{1}H NMR ($CDCl_2CDCl_2$, 400 MHz): δ: 8.77 (s, 2H), 7.27–7.36 (m, 8H), 7.10 (dd, J = 4.8 Hz, J = 3.6 Hz, 2H), 4.09 (d, J = 7.2 Hz, 4H), 1.98 (m, 2H), 1.16–1.45 (m, br, 64H), 0.80–0.90 (m, 12H).

Electrochemical thin film deposition

Electrochemical deposition of PNDI2ODT4, PEDOT and NDI2ODT4:EDOT copolymers has been performed by anodic oxidation of the monomers in a conventional three-electrode cell connected to a potentiostat/galvanostat (Metrohm Autolab PGSTAT 128N). No cathodic process has been observed for these systems. This is not surprising since thiophene derivatives have been usually observed to polymerize anodically.[38] Thin films have been prepared potentiodynamically by sweeping the applied potential in a range between the open circuit value and +1.3 V *vs.* Ag/AgCl, KCl (3.5 M) for 17 cycles at a scan rate of 50 mV s^{-1}. They have been deposited on both glassy carbon (GC, diameter = 3 mm, Bio-Logic SAS) and ITO/PET (35 Ω cm^{-2}, Sigma Aldrich) with different active areas. A graphite wire has been used as a counter electrode. Before each experiment, GC underwent a fine polishing procedure with 0.05 μm white alumina suspension in a polishing pad, followed by ultrasonication in de-ionized water and acetone respectively. ITO/PET electrodes have been cleaned in acetone using an ultrasonic bath. The electrodeposition solution has been carried out in 10^{-2} M lithium perchlorate ($LiClO_4$ purum ≥98%, Sigma Aldrich) in a mixture of acetonitrile (CH_3CN, anhydrous 99.8%, Sigma Aldrich) and dichloromethane (CH_2Cl_2, Chromasolv HPLC ≥99.8%, Sigma Aldrich) (2 : 3; v : v) containing a monomer concentration of 10^{-4} M and different molar ratios in the case of copolymers. All the experiments have been performed at room temperature. After the thin film electrodeposition, the modified working electrodes have been washed with a CH_3CN and CH_2Cl_2 mixture in order to remove the excess of both supporting electrolyte and monomers. The thin film thickness was estimated by Faraday's law and confirmed by measurements using a 3D Optical Profiler (Sensofar).

Computational details

The structural and electronic properties of all systems studied computationally in this work has been performed by means of density functional theory applying the oligomeric approach on a model where the computationally cumbersome alkyl chains of the NDI2ODT4 moiety have been substituted by methyl groups. The singlet–singlet adiabatic electronic transitions have been investigated by means of the time dependent density functional approach (TDDFT) by using the Coulomb-Attenuating Method applied to the B3LYP exchange–correlation functional (CAM-B3LYP)[30]

combined with the correlation consistent polarized valence double zeta (cc-pvdz) basis set. The calculation has been performed on the electronic ground state geometries, fully optimized at the same level of theory. The CAM-B3LYP functional is revealed to be a reliable choice for the calculation of singlet–singlet electronic transition energies in organic molecules,[31] and particularly for the case of charge-transfer transitions.[32] All calculations have been performed by employing the Gaussian 09 package.[33]

X-ray photoelectron spectroscopy (XPS)

Photoemission spectra were collected using a VG Microtech ESCA 3000 Multilab spectrometer, equipped with a standard Al Ka excitation source ($h\nu$ = 1486.6 eV) and a nine-channeltron detection system. The hemispherical analyser is operated in the CAE mode at a constant pass energy of 20 eV. The binding energy (BE) scale was calibrated by using the C 1s peak (BE = 285.1 eV) from the adventitious carbon and the accuracy of the measure was ±0.1 eV. The ultrahigh vacuum (UHV) analysis chamber was evacuated to a pressure value lower than 1×10^{-6} Pa during data collection. Photoemission data were collected and processed by using the VGX900 software. Data analysis was performed using a nonlinear least square curve-fitting program using a properly weighted sum of Lorentzian and Gaussian component curves and peak area determination after background subtraction according to Shirley and Sherwood procedures.[34,35] The surface chemical composition of the investigated samples was obtained by using the sensitivity factor approach,[36] based on peak area intensities calculated using a standard quantification routine, including Wagner's energy dependence of attenuation length,[37] and a standard set of VG Escalab sensitivity factors. The uncertainty on the atomic quantitative analysis is about ±10%.

Thin film characterization

Electrochemical behaviour of electrodeposited PNDI2ODT4, PEDOT and the NDI2ODT4:EDOT copolymer deposited on GC electrodes has been studied by means of cyclic voltammetry (CV) in CH_3CN containing 0.1 M $LiClO_4$ as a supporting electrolyte at room temperature. Morphological investigations of the surface have been carried out by using Scanning Electron Microscopy (SEM). SEM studies have been performed using a FEI FEG-ESEM (mod. QUANTA 200) at different voltages and magnifications. Gold has been sputtered onto the samples before the morphological analysis. Absorption spectra were recorded using a Beckman DU-640 spectrophotometer equipped with a 150 W xenon arc lamp as an excitation source. Spectroelectrochemical measurements have been performed by coupling both the Beckman DU-640 spectrophotometer and the Metrohm potentiostat/galvanostat. Two-electrode cell configuration has been used for this purpose. Transmittance *vs.* time plots under the applied square wave potential were recorded at the optimized wavelengths of 900 nm for PNDI2ODT4 and copol[1], 580 nm for copol[2], 588 nm for copol[3], and 600 nm for PEDOT. The response times have been calculated for about 100% of colour changes. The electrical measurements have been performed using a Keithley 4200-SCS Parameter Analyzer, configured in the voltage sweep mode. The metal contact with the organic thin layers electrodeposited on the ITO/PET substrate was realized with circular orifices through a polytetrafluoroethylene (PTFE) substrate filled with mercury (Hg). The Hg contact area was 0.05 cm^2. The voltage has been maintained positive whereas the Hg potential was higher than that of ITO.

AFM analysis

The surface morphology has been investigated by using an AFM Nanoscope V (Veeco Instruments Inc., Santa Barbara, California). Images (512 × 512 points, 1 Hz scan rate) have been acquired in dynamic-contact mode (Tapping Mode) by using silicon probes (RTESP-type, Veeco) with a nominal tip curvature of 10 nm.

Electrochromic device construction

Solid state electrochromic devices have been fabricated in a common sandwich configuration. NDI2ODT4:EDOT copolymer thin films electrodeposited on ITO/PET have been separated from ITO/PET counter electrodes by means of a transparent gel electrolyte. $LiClO_4$ (0.3 g) and poly(methyl methacrylate) (PMMA; M_w: 120 000 Sigma Aldrich) (0.7 g) have been dissolved in acetonitrile (7 g) and propylene carbonate (2 g) has been added as a plasticizer. The obtained gel electrolyte has been spread onto the polymeric film and finally the counter electrode has been added on the top.

Acknowledgements

Italian MiUR is acknowledged for funding through FIRB - Futuro in Ricerca (RBFR08DUX6) and PON R&C 2007–2013 (''TESEO'' – PON02_00153-2939517 and ''Plastic electronics for smart disposable systems'' – PON02_00355-3416798). AF thanks KAU for financial support.

Notes and references

1 (*a*) H. Sirringhaus, *Adv. Mater.*, 2005, **17**, 2411; (*b*) J. Smith, W. Zhang, R. Sougrat, K. Zhao, R. Li, D. Cha, A. Amassian, M. Heeney, I. McCulloch and T. D. Anthopoulos, *Adv. Mater.*, 2012, **24**, 2441; (*c*) H. Chen, Y. Guo, G. Yu, Y. Zhao, J. Zhang, D. Gao, H. Liu and Y. Liu, *Adv. Mater.*, 2012, **24**, 4618; (*d*) Z. He, C. Zhong, S. Su, M. Xu, H. Wu and Y. Cao, *Nat. Photonics*, 2012, **6**, 593; (*e*) R. Liu and S. B. Lee, *J. Am. Chem. Soc.*, 2008, **130**, 2942; (*f*) E. Bartollini, M. Seri, S. Tortorella, A. Facchetti, T. J. Marks, A. Marrocchi and L. Vaccaro, *RSC Adv.*, 2013, **3**, 9288; (*g*) A. Marrocchi, D. Lanari, A. Facchetti and L. Vaccaro, *Energy Environ. Sci.*, 2012, **5**, 8457; (*h*) K. Okamoto, J. Zhang, J. B. Housekeeper, S. R. Marder and C. K. Luscombe, *Macromolecules*, 2013, **46**(20), 8059; (*i*) M. Shao, J. Keum, J. Chen, Y. He, W. Chen, J. F. Browning, J. Jakowski, B. G. Sumpter, I. N. Ivanov, Y. Z. Ma, C. M. Rouleau, S. C. Smith, D. B. Geohegan,

K. Hong and K. Xiao, *Nat. Commun.*, 2014, **5**, DOI: 10.1038/ncomms4180.

2 (*a*) J. Roncali, *Macromol. Rapid Commun.*, 2007, **28**, 1761; (*b*) P. M. Beaujuge, S. Ellinger and J. R. Reynolds, *Nat. Mater.*, 2008, **7**, 795; (*c*) C. B. Nielsen, A. Angerhofer, K. A. Abboud and J. R. Reynolds, *J. Am. Chem. Soc.*, 2008, **130**, 9734.

3 (*a*) Y. Ie, T. Sakurai, S. Jinnai, M. Karakawa, K. Okunda, S. Mori and Y. Aso, *Chem. Commun.*, 2013, **49**, 8386; (*b*) I. V. Sazanovich, M. A. H. Alamiry, J. Best, R. D. Bennet, O. V. Bouganov, E. S. Davies, V. P. Grivin, A. J. H. M. Meijer, V. F. Plyusnin, K. L. Ronayne, A. H. Skelton, S. A. Tikhomirov, M. Towrie and J. A. Weinstein, *Inorg. Chem.*, 2008, **47**(22), 10432; (*c*) L. J. Rozanski, E. Castaldelli, F. L. M. Sam, C. A. Mills, G. J. F. Demets and S. R. P. Silva, *J. Mater. Chem. C*, 2013, **1**, 3347; (*d*) S. Fabiano, H. Wang, C. Piliego, C. Jaye, D. A. Fischer, Z. Chen, B. Pignataro, A. Facchetti, Y. L. Loo and M. A. Loi, *Adv. Funct. Mater.*, 2011, **21**, 4479.

4 (*a*) Y. Kim, J. Hong, J. H. Oh and C. Yang, *Chem. Mater.*, 2013, **25**, 3251; (*b*) H. Yan, Z. Chen, Y. Zheng, C. Newman, J. R. Quinn, F. Dötz, M. Kastler and A. Facchetti, *Nature*, 2009, **457**, 679; (*c*) A. Facchetti, *Chem. Mater.*, 2011, **23**, 733.

5 R. Kim, P. S. K. Amegadze, I. Kang, H. J. Yun, Y. Y. Noh, S. K. Kwon and Y. H. Kim, *Adv. Funct. Mater.*, 2013, **23**, 5719.

6 (*a*) X. Guo and M. D. Watson, *Org. Lett.*, 2008, **10**, 5333; (*b*) M. M. Durban, P. D. Kazarinoff and C. K. Luscombe, *Macromolecules*, 2010, **43**, 6348; (*c*) F. S. Kim, X. Guo, M. D. Watson and S. A. Jenekhe, *Adv. Mater.*, 2010, **22**, 478; (*d*) X. Guo, F. S. Kim, M. J. Seger, S. A. Jenekhe and M. D. Watson, *Chem. Mater.*, 2012, **24**, 1434; (*e*) M. Yuan, M. M. Durban, P. D. Kazarinoff, D. F. Zeigler, A. H. Rice, Y. Segawa and C. K. Luscombe, *J. Polym. Sci., Part A: Polym. Chem.*, 2013, **51**(19), 4061–4069; (*f*) A. Luzio, D. Fazzi, D. Natali, E. Giussani, K. J. Baeg, Z. Chen, Y. Y. Noh, A. Facchetti and M. Caironi, *Adv. Funct. Mater.*, 2014, **24**, 1151.

7 S. Fabiano, Z. Chen, S. Vahedi, A. Facchetti, B. Pignataro and M. A. Loi, *J. Mater. Chem.*, 2011, **21**, 5891.

8 N.-K. Kim, D. Khim, Y. Xu, S.-H. Lee, M. Kang, J. Kim, A. Facchetti, Y.-Y. Noh and D.-Y. Kim, *ACS Appl. Mater. Interfaces*, 2014, **6**(12), 9614.

9 (*a*) H. Krüger, S. Janietz, D. Sainova, D. Dobreva, N. Koch and A. Vollmer, *Adv. Funct. Mater.*, 2007, **17**, 3715; (*b*) M. Greenman, A. J. Ben-Sasson, Z. Chen, A. Facchetti and N. Tessler, *Appl. Phys. Lett.*, 2013, **103**, 073502.

10 R. Kim, P. S. K. Amegadze, I. Kang, H. J. Yun, Y. Y. Noh, S. K. Kwon and Y. H. Kim, *Adv. Funct. Mater.*, 2013, **23**, 5719.

11 J. Roncali, P. Blanchard and P. Frére, *J. Mater. Chem.*, 2005, **15**, 1589.

12 (*a*) G. A. Sotzing, C. A. Thomas and J. R. Reynolds, *Macromolecules*, 1998, **31**, 3750; (*b*) C. A. Thomas and J. R. Reynolds, in *ACS Symposium Series 735*, ed. B. R. Hsieh and Y. Wei, ACS, Washington DC, 1998, 367; (*c*) S. Akoudad and J. Roncali, *Chem. Commun.*, 1998, 2081.

13 H. Meng, D. Tucker, S. Chaffins, Y. Chen, R. Helgeson, B. Dunn and F. Wudl, *Adv. Mater.*, 2003, **15**, 147.

14 (*a*) M. Sassi, M. M. Salamone, R. Ruffo, C. M. Mari, G. A. Pagani and L. Beverina, *Adv. Mater.*, 2012, **24**, 2004; (*b*) J. Cai, L. Ma, H. Niu, P. Zhao, Y. Lian and W. Wang, *Electrochim. Acta*, 2013, **112**, 59; (*c*) T. Yijie, C. Haifeng, Z. Zhaoyang, X. Xiaoqian and Z. Yongjiang, *J. Electroanal. Chem.*, 2013, **689**, 142.

15 (*a*) G. A. Yiseen, *Int. J. Electrochem. Sci.*, 2014, **9**, 2575; (*b*) G. A. Sotzing, J. R. Reynolds and P. J. Steel, *Adv. Mater.*, 1991, **9**(10), 795.

16 (*a*) P. Leriche, P. Blanchard, P. Frère, E. Levillain, G. Mabon and J. Roncali, *Chem. Commun.*, 2006, 275; (*b*) J. Roncali, P. Blanchard and P. Frère, *J. Mater. Chem.*, 2005, **15**, 1589.

17 R. Steyleuthner, M. Schubert, I. Howard, B. Klaumünzer, K. Schilling, Z. Chen, P. Sallfrank, F. Laquai, A. Facchetti and D. Neher, *J. Am. Chem. Soc.*, 2012, **134**, 18303.

18 D. K. Seo and R. Hoffmann, *Theor. Chem. Acc.*, 1999, **102**, 23.

19 G. Sonmez and H. B. Sonmez, *J. Mater. Chem.*, 2006, **16**, 2473.

20 Y. Kim, J. Hong, J. H. Oh and C. Yang, *Chem. Mater.*, 2013, **25**, 3251.

21 Y. Wei, Q. Zhang, Y. Jiang and J. Yu, *Macromol. Chem. Phys.*, 2009, **210**, 769.

22 (*a*) J. Xia, N. Masaki, M. Lira-Cantu, Y. Kim, K. Jiang and S. Yanagida, *J. Am. Chem. Soc.*, 2008, **130**(4), 1258; (*b*) V. Castagnola, C. Bayon, E. Descamps and C. Bergaud, *Synth. Met.*, 2014, **189**, 7.

23 R. Steyrleuthner, M. Schubert, F. Jaiser, J. C. Blakesley, Z. Chen, A. Facchetti and D. Neher, *Adv. Mater.*, 2010, **22**, 2799.

24 T. Yi-Jie, C. Hai-Feng, Z. Wen-Wei and Z. Zhao-Yang, *J. Appl. Polym. Sci.*, 2013, 636.

25 S. Hsiao, P. Chang, H. Wang, Y. Kung and T. Lee, *J. Polym. Sci., Part A: Polym. Chem.*, 2014, **52**, 825.

26 J. Cai, L. Ma, H. Niu, P. Zhao, Y. Lian and W. Wang, *Electrochim. Acta*, 2013, **112**, 59.

27 P. M. S. Monk, R. J. Mortimer and D. R. Rosseinsky, *Electrochromism and Electrochromic devices*, Cambridge University Press, 2007.

28 E. G. Tolstopyatova, N. A. Pogulaichenko, S. N. Eliseeva and V. V. Kondratiev, *Russ. J. Electrochem.*, 2009, **45**(3), 252.

29 T. Yijie, C. Haifeng, Z. Zhaoyang, X. Xiaoqian and Z. Yongjiang, *J. Electroanal. Chem.*, 2013, **689**, 142.

30 T. Yanai, D. Tew and N. Handy, *Chem. Phys. Lett.*, 2004, **393**, 51.

31 (*a*) D. Jacquemin, V. Wathelet, E. A. Perpete and C. Adamo, *J. Chem. Theory Comput.*, 2009, **5**, 2420; (*b*) S. Kupfer, J. Guthmuller and L. González, *J. Chem. Theory Comput.*, 2013, **9**, 543.

32 M. J. G. Peach, A. J. Cohen and D. J. Tozer, *Phys. Chem. Chem. Phys.*, 2006, **8**, 4543.

33 M. J. Frisch, G. W. Trucks, H. B. Schlegel, G. E. Scuseria, M. A. Robb, J. R. Cheeseman, G. Scalmani, V. Barone, B. Mennucci, G. A. Petersson, H. Nakatsuji, M. Caricato, X. Li, H. P. Hratchian, A. F. Izmaylov, J. Bloino, G. Zheng, J. L. Sonnenberg, M. Hada, M. Ehara, K. Toyota, R. Fukuda, J. Hasegawa, M. Ishida, T. Nakajima, Y. Honda, O. Kitao,

H. Nakai, T. Vreven, J. A. Montgomery Jr., J. E. Peralta, F. Ogliaro, M. Bearpark, J. J. Heyd, E. Brothers, K. N. Kudin, V. N. Staroverov, R. Kobayashi, J. Normand, K. Raghavachari, A. Rendell, J. C. Burant, S. S. Iyengar, J. Tomasi, M. Cossi, N. Rega, J. M. Millam, M. Klene, J. E. Knox, J. B. Cross, V. Bakken, C. Adamo, J. Jaramillo, R. Gomperts, R. E. Stratmann, O. Yazyev, A. J. Austin, R. Cammi, C. Pomelli, J. W. Ochterski, R. L. Martin, K. Morokuma, V. G. Zakrzewski, G. A. Voth, P. Salvador, J. J. Dannenberg, S. Dapprich, A. D. Daniels, Ö. Farkas, J. B. Foresman, J. V. Ortiz, J. Cioslowski and D. J. Fox, *Gaussian 09, Revision C.01*, Gaussian, Inc., Wallingford CT, 2009.

34 D. Briggs, *Surface analysis of polymers by XPS and static SIMS*, Cambridge University Press, Cambridge, U.K., 1998.

35 (*a*) D. A. Shirley, *Phys. Rev. B: Solid State*, 1972, **5**, 4709; (*b*) P. M. A. Sherwood, Data Analysis in X-ray Photoelectron Spectroscopy, in *Practical Surface Analysis by Auger and X-ray Photoelectron Spectroscopy*, ed. D. Briggs and M. P. Seah, Wiley, New York, 1983, pp. 445–474.

36 C. D. Wagner, L. E. Davis, M. V. Zeller, J. A. Taylor, R. H. Raymond and L. H. Gale, *Surf. Interface Anal.*, 1981, **3**, 211.

37 C. D. Wagner, L. E. Davis and W. M. Riggs, *Surf. Interface Anal.*, 1980, **2**, 53.

38 J. Heinze, B. A. Frontana Uribe and S. Ludwigs, *Chem. Rev.*, 2010, **110**, 4724.